Supporting Information

Concentration-Dependent, Supramolecular Interconversions of Triptycene-Based Cube, Prism, and Tetrahedron Structures

Sourav Chakraborty,[a] Kevin J. Endres,[a] Ranajit Bera,[c] Lukasz Wojtas,[d] Charles N. Moorefield,[e] Mary Jane Saunders,[f] Neeladri Das,[c] Chrys Wesdemiotis,*[a,b] and George R. Newkome*[a,b,g]

[a]Department of Polymer Science and [b]Department of Chemistry, The University of Akron, Akron, Ohio 44325, USA.

[c]Department of Chemistry, Indian Institute of Technology Patna, Patna 801106, Bihar, India

[d]Department of Chemistry, University of South Florida, 4202 East Fowler Avenue, Tampa, Florida 33620, USA.

[e]Dendronix LLC, 109 Runway Dr., Reese Technology Center, Lubbock TX 79424, USA

[f]Department of Biological Sciences, Florida Atlantic University, Boca Raton, Florida 33431, USA.

[g]Center for Molecular Biology and Biotechnology, Florida Atlantic University, 5353 Parkside Drive, Jupiter, Florida 33458, USA

E-mail: wesdemiotis@uakron.edu, newkome@uakron.edu

Table of Contents **Page(s)**

Experimental Section.

General Procedures. Reagents and solvents were purchased from Sigma-Aldrich and used without purification. Thin layer chromatography (TLC) was performed on flexible sheets (Baker-flex) precoated with Al_2O_3 (IB-F) or SiO_2 (IB2-F) and visualized by UV light. Column chromatography was conducted using basic Al_2O_3, Brockman Activity I (60-325 mesh) or SiO_2 (60-200 mesh) from Fisher Scientific. ^1H, ^{13}C, 2D COSY, and NOESY NMR spectra were recorded on a Varian NMR 500 (MHz).

ESI mass spectrometry (MS) experiments were performed on a Waters Synapt HDMS quadrupole/time-of-flight (Q/ToF) tandem mass spectrometer, containing a triwave device between the Q and ToF analyzers, consisting of three collision cells in the order: trap cell, ion mobility cell, and transfer cell. Trap and transfer cells are pressurized with Ar, and the ion mobility cell is pressurized with N_2 flowing in a direction opposite to that of the entering ions. D-Ala^2-Leucine Enkephalin was used to calibrate all ESI mass spectra. In the TWIM-MS experiments, a pulsed field is applied to the ion mobility cell ("traveling wave" field) to separate the ions drifting inside it by their charge state and collision cross-section. The proteins, used to calibrate the drift time scale in the TWIM-MS experiments to obtain the collision cross-section data, were acquired from Sigma-Aldrich. The ESI-TWIM-MS experiments were performed using the following parameters: ESI capillary voltage: 3.2 kV; sample cone voltage: 15 V; extraction cone voltage: 0.5 V; desolvation gas flow: 500 L/h (N_2); trap collision energy (CE): 6 eV; transfer CE: 4 eV; trap gas flow: 1.5 mL/min (Ar); ion-mobility cell gas flow: 22.7 mL/min (N_2); sample flow rate: 5μL/min; source temperature: 70 °C; desolvation temperature: 150 °C; TWIM traveling-wave height: 7.5 V; and TWIM traveling-wave velocity: 350 ms^{-1}. The sprayed solution was prepared by dissolving the sample in MeCN. Data analyses were conducted using the MassLynx 4.1 and DriftScope 2.1 programs provided by Waters. Theoretical collision cross sections were calculated from energy minimized structures using the trajectory method available in the MOBCAL software.

For the TEM investigation, the sample was dissolved in MeCN at a concentration within the 10^{-6} to 10^{-7} M range. The solution was drop cast onto a carbon-coated copper grid and any extra solution was absorbed by filter paper to avoid aggregation. The TEM images of the drop cast samples were taken with a Jeol JEM-1230 transmission electron microscope.

Collision Cross-Section Calibration. The drift time scale of the TWIM-MS experiments was converted to a collision cross-section scale, following the calibration procedure of Scrivens *et al*.[1] Briefly, the corrected collision cross-sections of the molecular ions of cytochrome-C (equine heart) were obtained from published work,[2] plotted against the corrected drift times (arrival times) of the corresponding molecular ions measured in TWIM-MS experiments at the same traveling-wave velocity, traveling-wave height, and ion-mobility gas flow settings, *viz.* 350 ms^{-1}, 7.5 V, and 22.7 mL/min. Charge states, observed for the calibrant from 9+ to 19+, were used in the construction of the curve.

Molecular Modeling. Energy minimization of these structures was conducted with the Materials Studio version 6.0 program using the Anneal and Geometry Optimization tasks in the Forcite module (Accelrys Software, Inc.). The counterions were omitted. An initially energy-minimized structure was subjected to 20 annealing cycles with initial and mid-cycle temperatures of 300 and 1500 K, respectively, five heating ramps per cycle, one hundred dynamics steps per ramp, and one dynamics step per femtosecond. A constant volume/constant energy (NVE) ensemble was used; the geometry was optimized after each cycle. All geometry optimizations used a universal force field with atom-based summation and cubic spline truncation for both the electrostatic and van der Waals parameters. 100 Candidate structures were generated for the calculation of collision cross sections.

Single-Crystal X-Ray Diffraction: The X-ray diffraction data for **4** were collected using synchrotron radiation (λ = 0.44281 Å) at Advanced Photon Source Beamline 15-ID-B of ChemMatCARS in Argonne National Laboratory, Argonne, IL. Indexing was performed in Apex3 software.[3] Data integration and reduction were performed using SaintPlus.[4] Absorption correction was performed by multi-scan method implemented in SADABS.[5] Space group was determined using XPREP implemented in APEX2.[3] Structure was solved using SHELXT[6] and refined using SHELXL-2014[7-9] (full-matrix least-squares on F2) through OLEX2 interface program.[10] All non-hydrogen atoms were refined anisotropically. All hydrogen atoms were placed in geometrically calculated positions and were included in the refinement process using the riding model with isotropic thermal parameters. The diffraction spots were observed only up to *ca*. 1.2-1.3Å resolution and all atoms were refined with geometry and ADP restraints. The model of the crystal structure was refined in I-43c space group. Attempts to refine the model in Im-3c space group resulted in the presence of massive disorder of the ligand due to the extra symmetry. The contribution of heavily disordered solvent molecules in structural voids was treated as diffuse using Squeeze procedure implemented in the Platon program.[11,12] The Squeeze procedure was run twice, first on original data and then on the Squeezed data. Only original data were included in CIF file. Crystal data and refinement conditions are shown in Table S7.

***Tris*-2,7,14-[4'-terpyridinyl]triptycene (Monomer 3).**

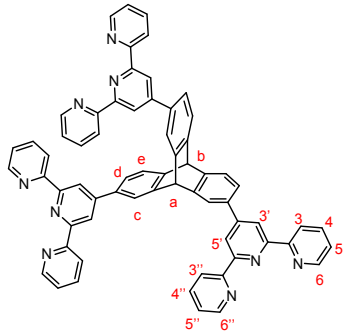

2,7,14-Tribromotriptycene[12] (**1**; 122 mg, 250 µmol), ([2,2':6',2"]terpyridin-4'-yl)boronic acid [13] (**2**; 415 mg, 1.5 mmol), Na_2CO_3 (552 mg, 4.0 mmol), and $PdCl_2(PPh_3)_2$ (52 mg, 75 mol) were dissolved in a mixture of toluene (200 mL), H_2O (120 mL), and EtOH (80 mL). The resultant solution was refluxed for 24 h under N_2. After cooling to 25 °C, the aqueous layer was extracted with $CHCl_3$ (3 × 100 mL) and the combined organic phase was dried over anh. $MgSO_4$, then concentrated *in vacuo* to give a crude organic phase that was column chromatographed (Al_2O_3) eluting with a mixture of $CHCl_3$, hexane, and EtOAc (1:2:1, v/v/v) to give **3**, as a white solid: 178 mg (75%); m.p. 233-235 °C; ^{1}H NMR (500 MHz, $CDCl_3$, ppm, Figure S1): δ 8.77–8.74 (m, 6H, tpy$H^{6,6"}$), 8.73 (s, 6H, tpy$H^{3',5'}$), 8.66 (d, J = 7.9 Hz, 6H, tpy$H^{3,3"}$), 8.08 (s, 3H, PhH^{c}), 7.86 (td, J = 7.7, 1.8 Hz, 6H, tpy$H^{4,4"}$), 7.65 (dd, J = 7.7, 1.6 Hz, 3H, PhH^{e}), 7.61 (d, J = 7.7 Hz, 3H, PhH^{d}), 7.37–7.31 (m, 6H, tpy$H^{5,5"}$), 5.85 (s, 1H, CH^{a}), 5.67 (s, 1H, CH^{b}); ^{13}C NMR (125 MHz, $CDCl_3$, ppm, Figure S3): δ 156.3, 155.8, 150.0, 149.1, 145.7, 145.5, 136.7, 136.0, 124.8, 124.2, 123.6, 122.9, 121.2, 118.8, 54.3, 53.4; MALDI-MS (m/z), Figure S4: m/z = 948.29 for [**3**+H]$^+$.

Synthesis of Cube 4.

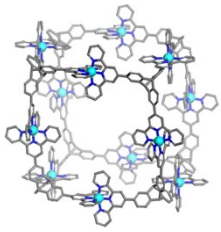

To a solution of tetra*kis*terpyridinyl ligand **3** (7.5 mg, 8 µmol) in $CHCl_3$ and MeOH (1:1, 16 mL), a MeOH (1 mL) solution of $Zn(NO_3)_2{\cdot}6H_2O$ (3.5 mg, 12 µmol) was slowly added. The mixture was stirred at 25 ºC for 2h, then a 10-fold excess NH_4PF_6 was added. The residue was filtered, washed with water (10 mL × 3) and MeOH (10 mL × 3), and lastly dried *in vacuo* to give quantitatively cube **4**, as a white solid: m.p. >400 °C; ^{1}H NMR (500 MHz, CD_3CN, ppm, Figure S5): δ 9.03 (s, 48H, tpy$H^{3',5'}$), 8.82 (d, J = 8.2 Hz, 48H, tpy$H^{3,3"}$), 8.36 (s, 24H, PhH^{c}), 8.17 (t, J = 7.9 Hz, 48H, tpy$H^{4,4"}$), 8.03 (d, J = 7.8 Hz, 24H, PhH^{e}), 7.97 – 7.85 (m, 72H,

tpy$H^{6,6''}$, PhH^{d}), 7.42 (dd, J = 7.3, 5.5 Hz, 48H, tpy$H^{5,5''}$), 6.29 (s, 8H, CH^{a}), 6.28 (s, 8H, CH^{b}); ^{13}C NMR (125 MHz, CD_3CN, ppm, Figure S8): δ 157.1, 149.6, 147.9, 147.8, 147.0, 146.3, 141.2, 134.9, 127.5, 126.0, 125.3, 124.4, 123.2, 122.2, 53.7, 52.8; ESI-MS (*m/z*), Figure S9: 1829.50 [**4** – 6 PF_6^-]$^{6+}$, 1447.65 [**4** – 7 PF_6^-]$^{7+}$, 1336.08 [**4** – 8 PF_6^-]$^{8+}$, 1171.52 [**4** – 9 PF_6^-]$^{9+}$, 1039.76 [**4** – 10 PF_6^-]$^{10+}$, 932.06 [**4** – 11 PF_6^-]$^{11+}$, 842.47 [**4** – 12 PF_6^-]$^{12+}$, 766.36 [**4** – 13 PF_6^-]$^{13+}$, 701.27 [**4** – 14 PF_6^-]$^{14+}$, 644.91 [**4** – 15 PF_6^-]$^{15+}$, 595.61 [**4** – 16 PF_6^-]$^{16+}$.

Synthesis of Cube 5.

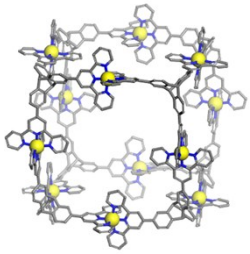

The above procedure, as described for **4**, was used, except utilizing $Cd(NO_3)_2$, followed by NH_4PF_6 anion exchange, to give (98%) the desired Cd complex **5**, as a white solid: m.p. >400 °C; ^{1}H NMR (500 MHz, CD_3CN, ppm, Figure S12): δ 8.93 (s, 48H, tpy$H^{3',5'}$), 8.81 (d, J = 8.0 Hz, 48H, tpy$H^{3,3''}$), 8.35 (s, 24H, PhH^{c}), 8.22 (t, J = 7.4 Hz, 48H, tpy$H^{4,4''}$), 8.17 – 8.09 (m, 48H, tpy$H^{6,6''}$), 8.00 (d, J = 7.7 Hz, 24H, PhH^{e}), 7.90 (d, J = 7.4 Hz, 24H, PhH^{d}), 7.56 – 7.45 (m, 48H, tpy$H^{5,5''}$), 6.32 (s, 8H, CH^{a}), 6.23 (s, 8H, CH^{b}); ^{13}C NMR (125 MHz, CD_3CN, ppm, Figure S15): δ 156.0, 150.2, 149.6, 148.7, 146.9, 146.3, 141.2, 134.8, 127.3, 126.0, 125.2, 124.3, 123.7, 122.4, 53.5, 52.7; ESI-MS (*m/z*), Figure S16: 2957.57 [**5** – 4 PF_6^-]$^{4+}$, 2337.50 [**5** – 5 PF_6^-]$^{5+}$, 1924.00 [**5** – 6 PF_6^-]$^{6+}$, 1628.49 [**5** – 7 PF_6^-]$^{7+}$, 1606.65 [**5** – 8 PF_6^-]$^{8+}$, 1234.24 [**5** – 9 PF_6^-]$^{9+}$, 1096.32 [**5** – 10 PF_6^-]$^{10+}$.

Complex (7) with PF_6^-:

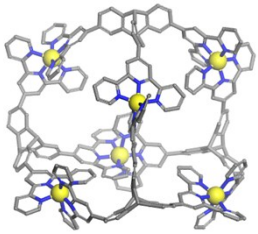

Dilution of a CD_3CN solution of complex **5** to 0.05 mg/mL gave the pure tetrahedron complex **7**: ^{1}H NMR (500 MHz, CD_3CN, ppm, Figure S19): δ 8.88 (s, 24H, tpy$H^{3',5'}$), 8.76 (d, J = 8.1 Hz, 24H, tpy$H^{3,3''}$), 8.32 – 8.14 (m, 36H, PhH^{c}, tpy$H^{4,4''}$), 8.08 – 7.91 (m, 48H, tpy$H^{6,6''}$, PhH^{e}, PhH^{d}), 7.60 – 7.53 (m, 24H, tpy$H^{5,5''}$), 6.22 (s, 4H, CH^{b}), 6.18 (s, 4H, CH^{a}); ESI-MS (*m/z*), Figure S21: 1923.91 [**7** – 3 PF_6^-]$^{3+}$, 1406.96 [**7** – 4 PF_6^-]$^{4+}$, 1096.37 [**7** – 5 PF_6^-]$^{5+}$, 889.30 [**7** – 6 PF_6^-]$^{6+}$, 741.54 [**7** – 7 PF_6^-]$^{7+}$, 630.60 [**7** – 8 PF_6^-]$^{8+}$, 544.65 [**7** – 9 PF_6^-]$^{9+}$.

Complex (6) with PF_6^-:

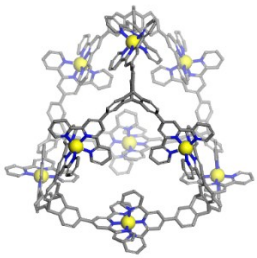

Dilution of the CD_3CN solution of complex **5** to 0.2 mg/mL gave a mixture of the prism complex **6** along with tetrahedron **7**: For prism **6**: ^1H NMR (500 MHz, CD_3CN, ppm, Figure S23): δ 8.92 (s, 12H, tpy^A*H*$^{3',5'}$), 8.89 (s, 24H, tpy^B*H*$^{3',5'}$), 8.82 – 8.77 (m, 36H, tpy^A*H*$^{3,3''}$, tpy^B*H*$^{3,3''}$), 8.32 (s, 18H, Ph*H*^{c}), 8.23 – 8.20 (m, 36H, tpy^A*H*$^{4,4''}$, tpy^B*H*$^{4,4''}$), 8.14 – 8.13 (m, 12H, tpy^A*H*$^{6,6''}$), 8.04 – 8.02 (m, 24H, tpy^B*H*$^{6,6''}$), 8.00 – 8.01 (m, 18H, Ph*H*^{e}), 7.91 – 7.88 (m, 18H, Ph*H*^{d}), 7.56 – 7.52 (m, 36H, tpy^A*H*$^{5,5''}$, tpy^B*H*$^{5,5''}$), 6.28 (s, 6H, C*H*^{a}), 6.22 (s, 6H, C*H*^{b}); ESI-MS (*m/z*), Figure S26: 2182.68 [**6** – 4 PF_6^-]$^{4+}$, 1717.00 [**6** – 5 PF_6^-]$^{5+}$, 1406.66 [**6** – 6 PF_6^-]$^{6+}$, 1184.99 [**6** – 7 PF_6^-]$^{7+}$, 1018.62 [**6** – 8 PF_6^-]$^{8+}$, 889.12 [**6** – 9 PF_6^-]$^{9+}$, 785.90 [**6** – 10 PF_6^-]$^{10+}$, 701.47 [**6** – 11 PF_6^-]$^{10+}$.

Procedures for the Variable Concentration Experiment

***Dilution*:** Cube **5** (12 mg) was dissolved in MeCN (1 mL, CD_3CN for NMR and MeCN for ESI-MS) to form a clear colorless solution (12 mg mL^{-1}). Then, 0.5 mL of this solution (12 mg mL^{-1}) was mixed with MeCN (0.1 mL, CD_3CN for NMR and MeCN for ESI-MS) to form a 10 mg mL^{-1} solution, which was immediately used to perform either the NMR or MS studies. All other diluted solutions were formed following the same procedure with addition of the respective amount of MeCN solvent.

***Concentration*:** A 5 mL sample of tetrahedron **7** in MeCN (0.05 mg mL^{-1}) was placed in a small glass vial, which was open to the air and evaporated at 30 °C in a water bath. The overall weight of the vial and solution was monitored using a balance. When the weight was reduced by 1.95 g (2.5 mL MeCN) and the concentration reached 0.1 mg mL^{-1}, the MS studies were conducted. All the other dilute solutions were formed following the same procedure with evaporation of the respective amount of MeCN solvent. It is obvious that concentration procedures were much slower than these for dilution.

NMR Spectra and Mass Spectral Data of Ligands and Complexes.

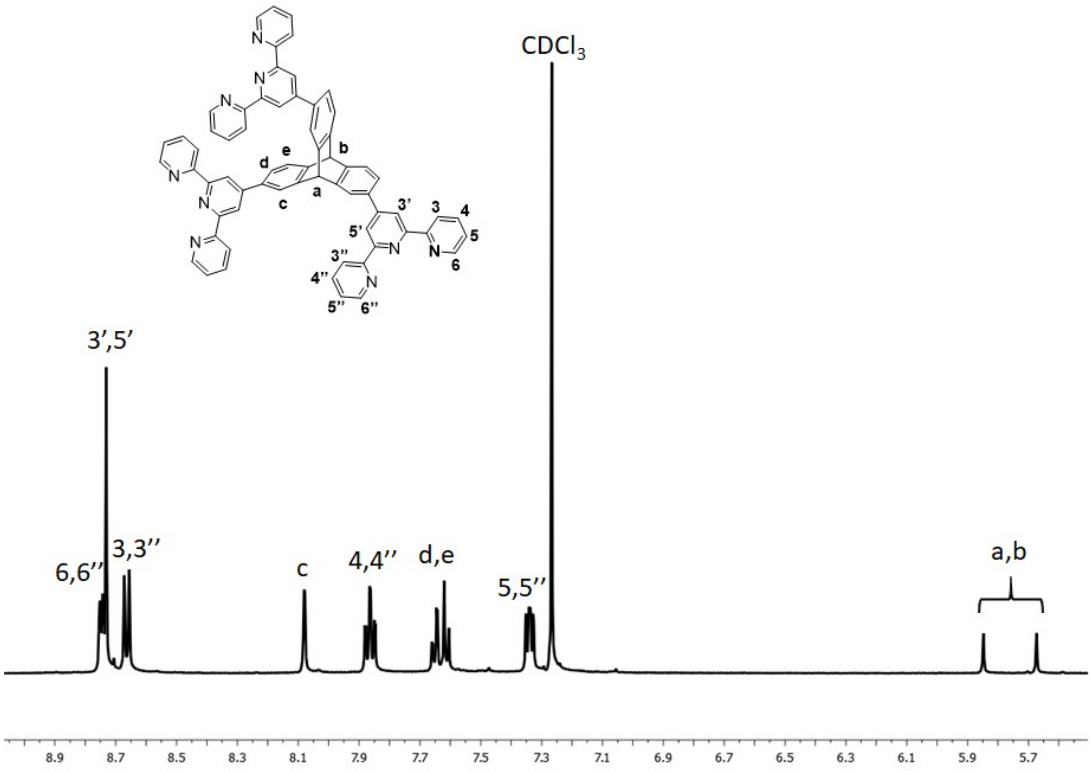

Figure S1. ^{1}H NMR spectrum (500 MHz, 300 K) of monomer **3** in $CDCl_3$.

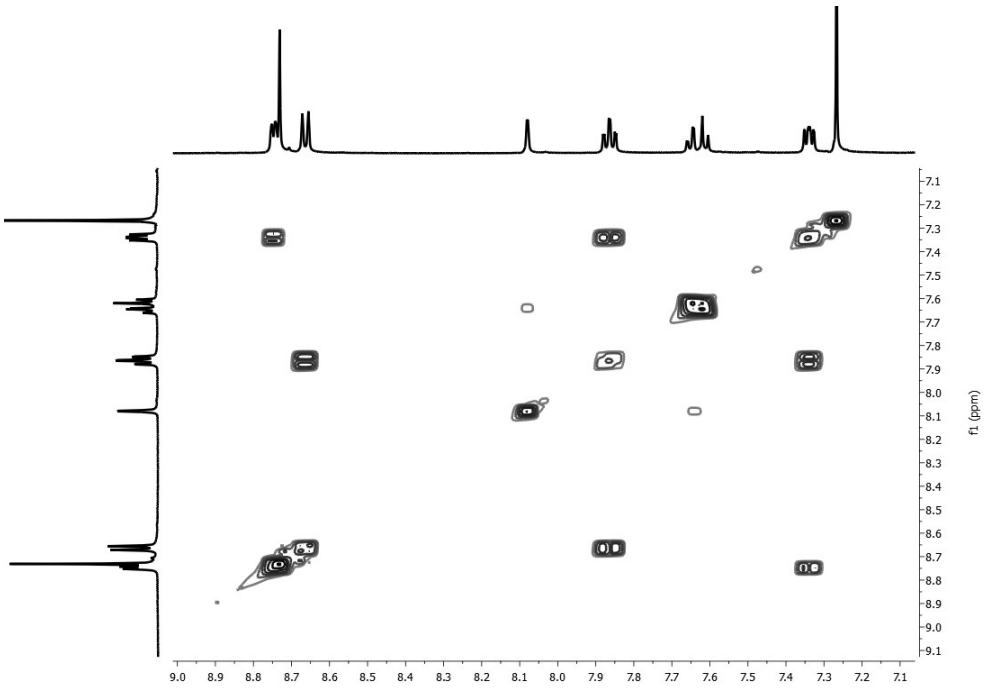

Figure S2. 2D COSY NMR spectrum of monomer **3** in $CDCl_3$.

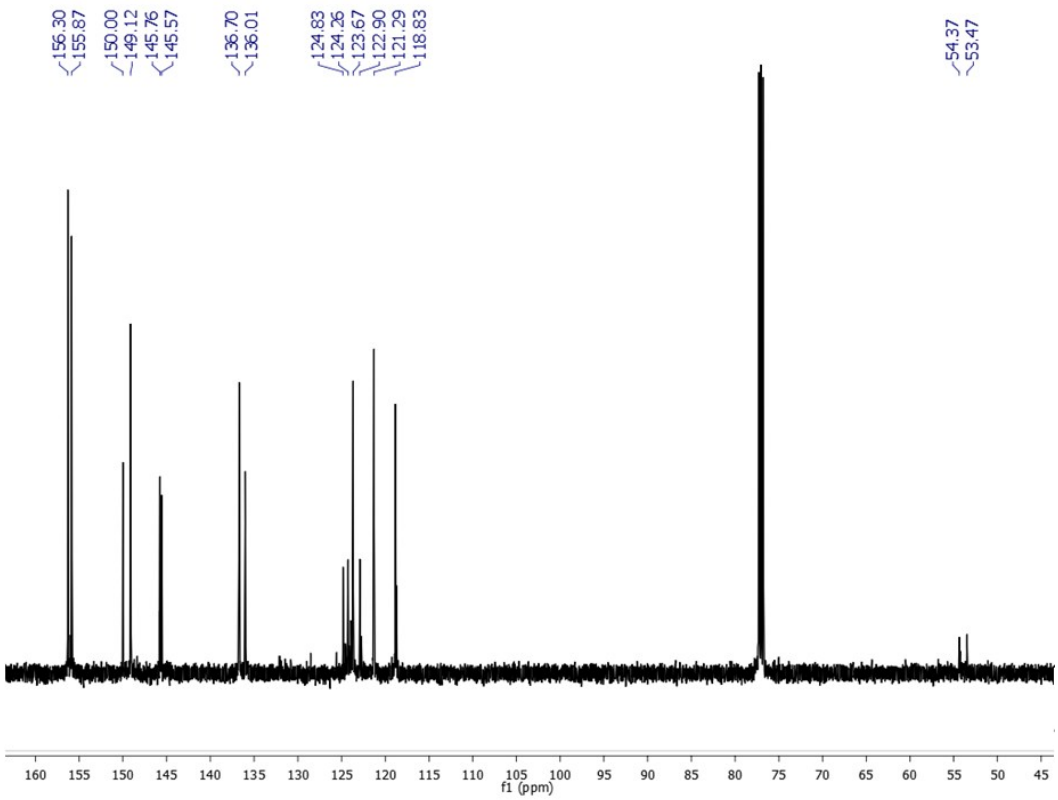

Figure S3. ^{13}C NMR spectrum (125 MHz, 300 K) of monomer **3** in $CDCl_3$.

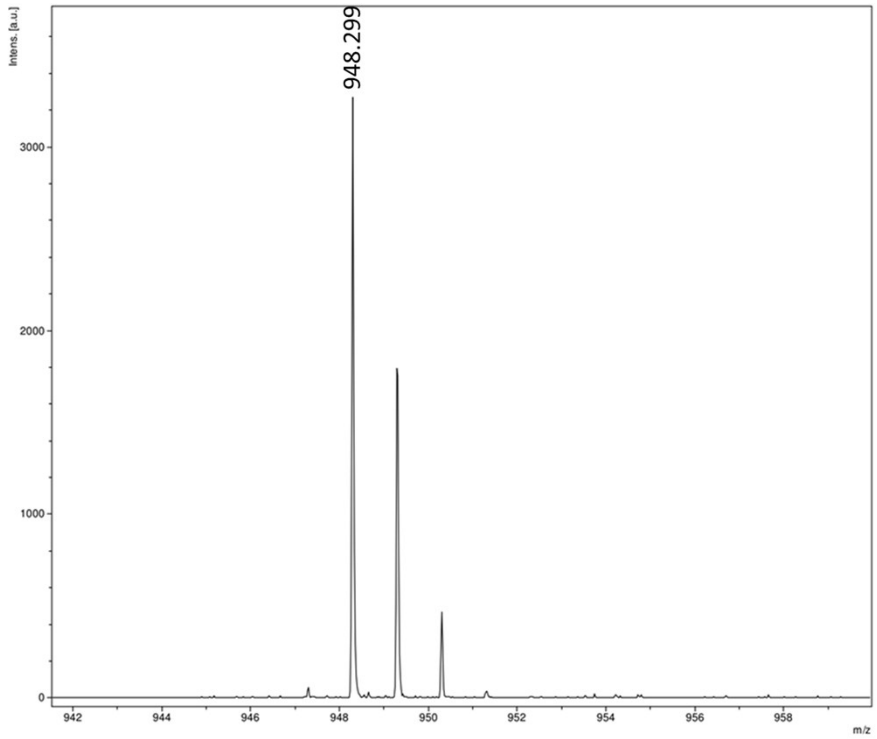

Figure S4. MALDI-MS spectrum of monomer **3**.

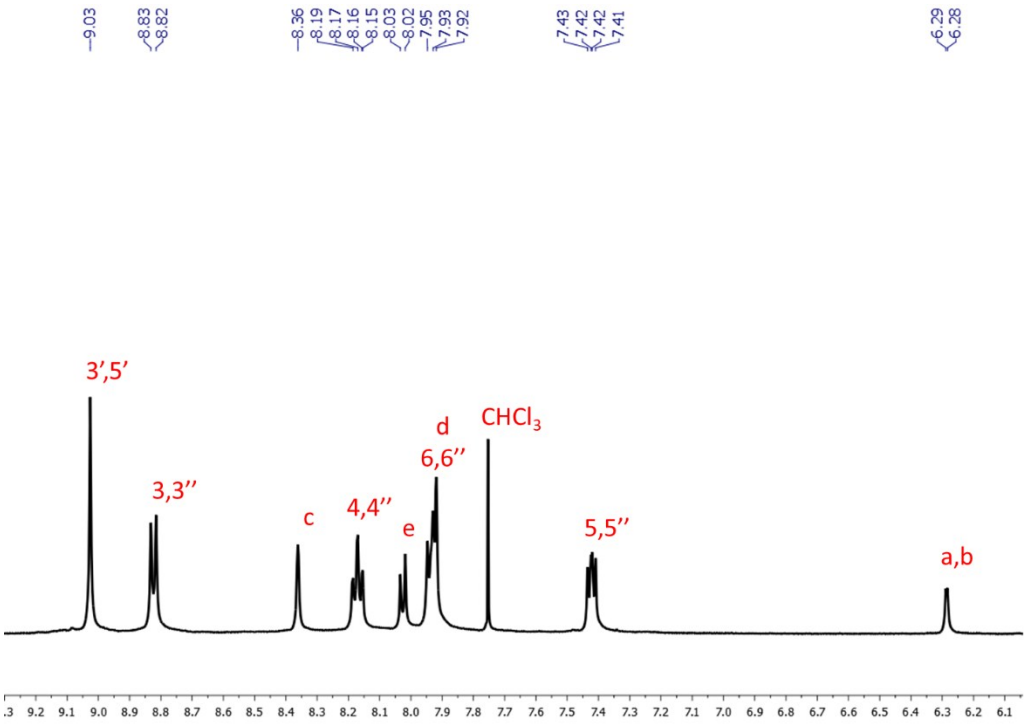

Figure S5. ^{1}H NMR spectrum (500 MHz, 300 K) of cube **4** in CD_3CN.

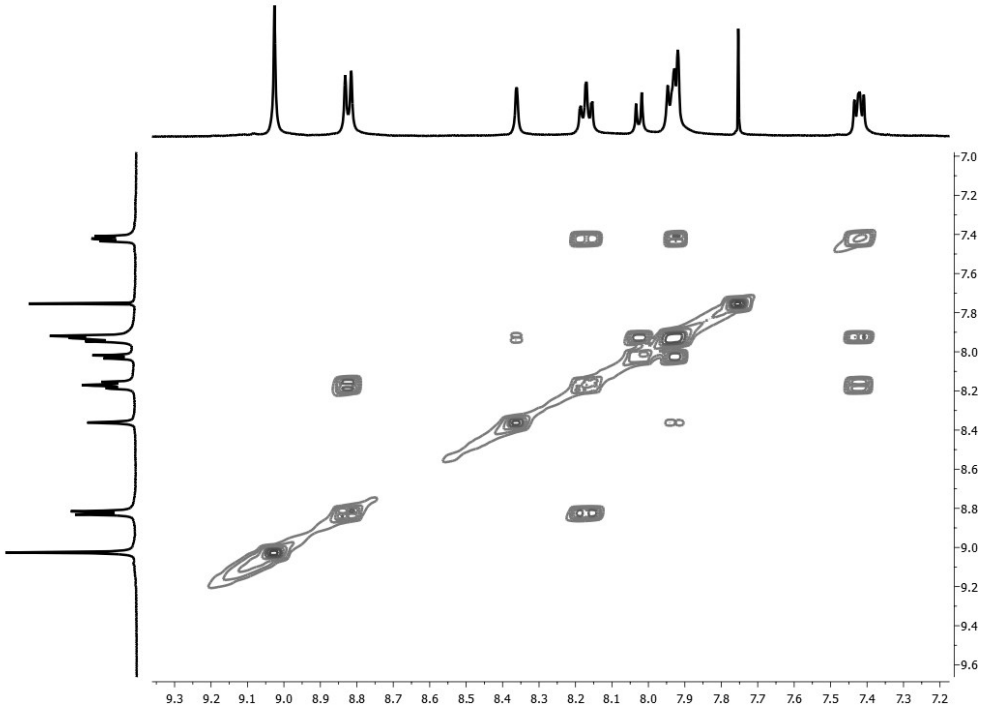

Figure S6. 2D COSY NMR spectrum of cube **4** in CD_3CN.

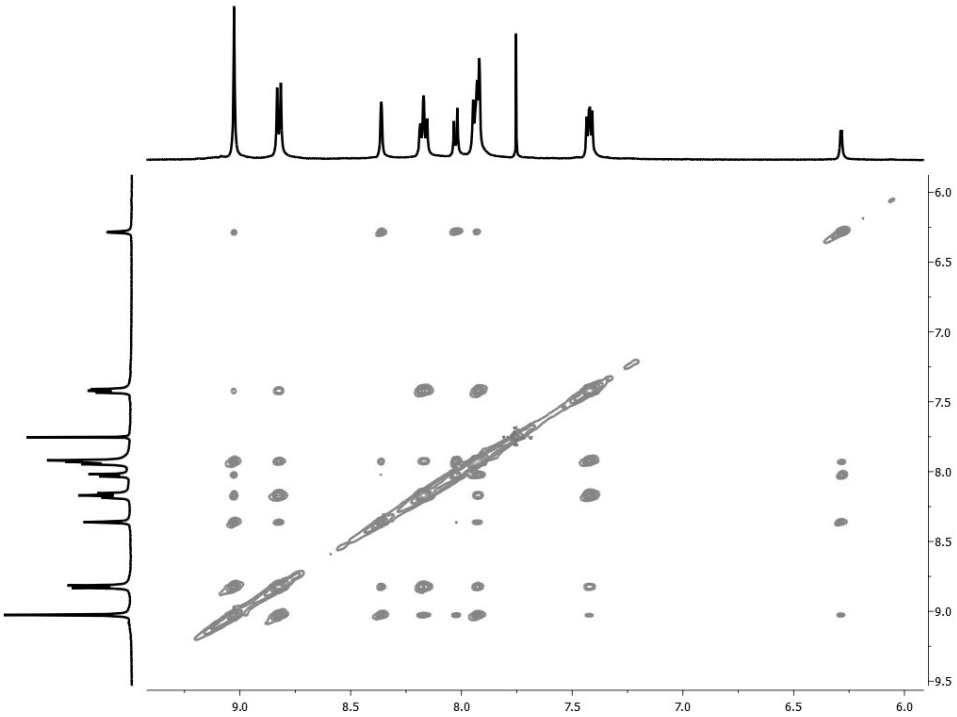

Figure S7. 2D NOESY NMR spectrum of cube **4** in CD_3CN.

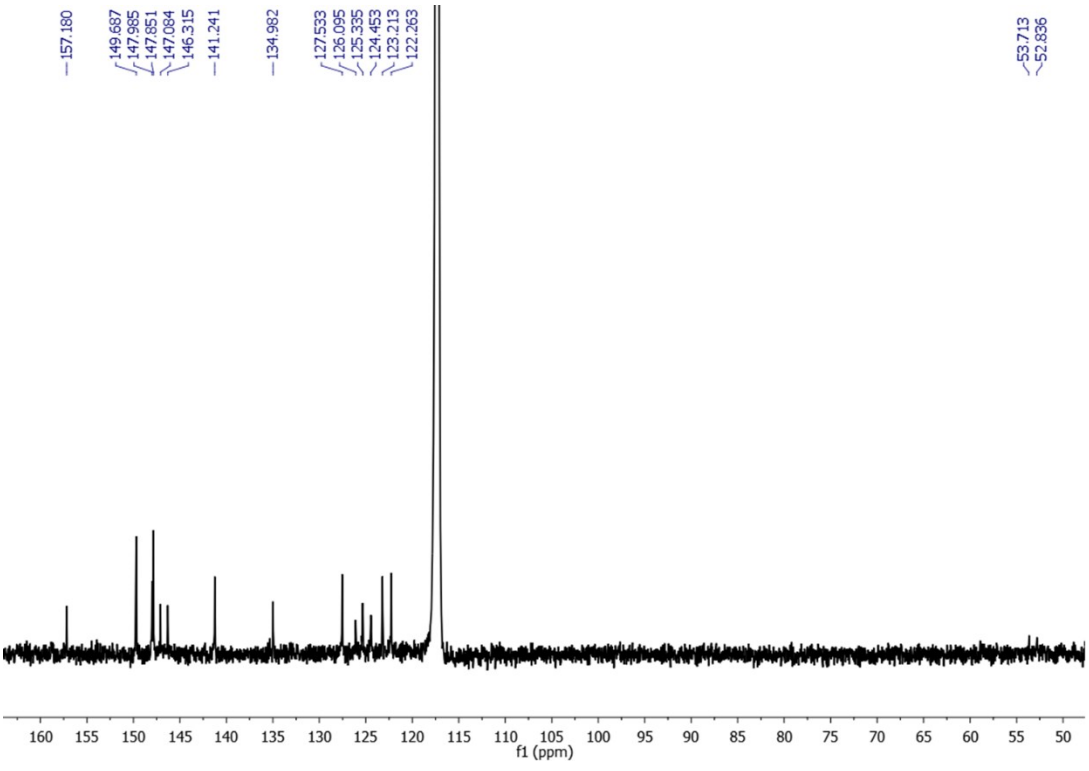

Figure S8. ^{13}C NMR spectrum (125 MHz, 300 K) of cube **4** in CD_3CN.

Stability of Zn^{2+} cube 4 at high dilution:

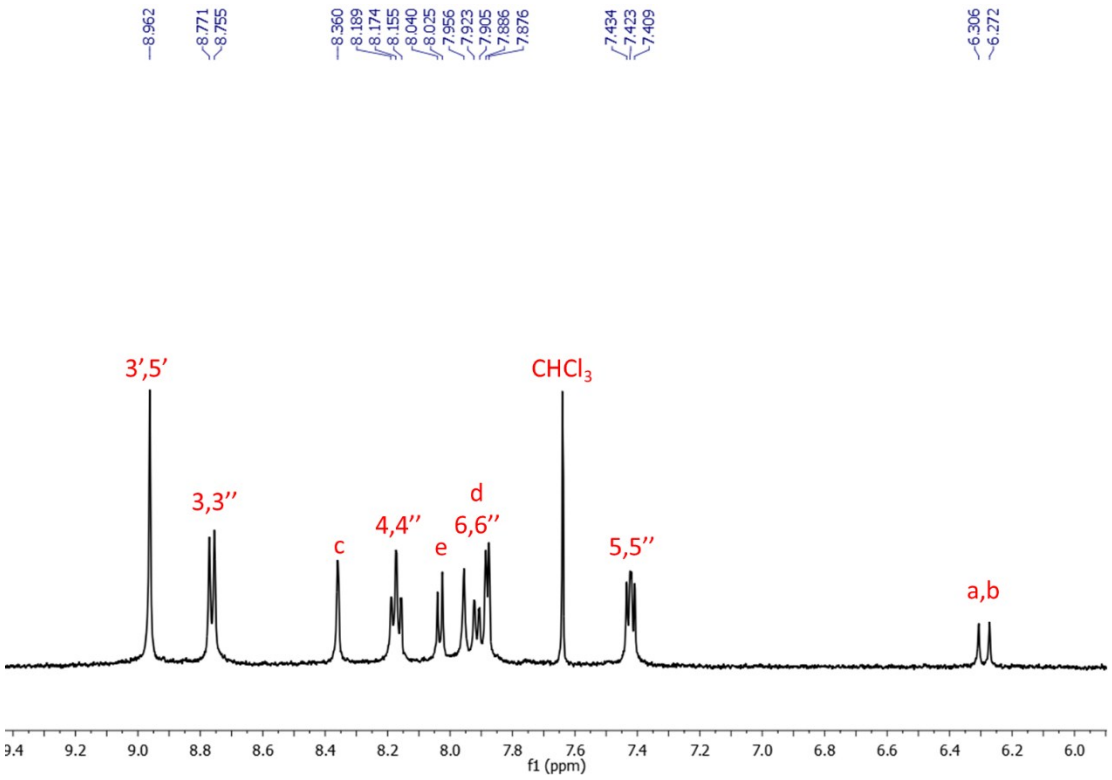

Figure S9. ^{1}H NMR spectrum (500 MHz, 300 K) of cube **4** in CD_3CN (0.1 mg mL^{-1}).

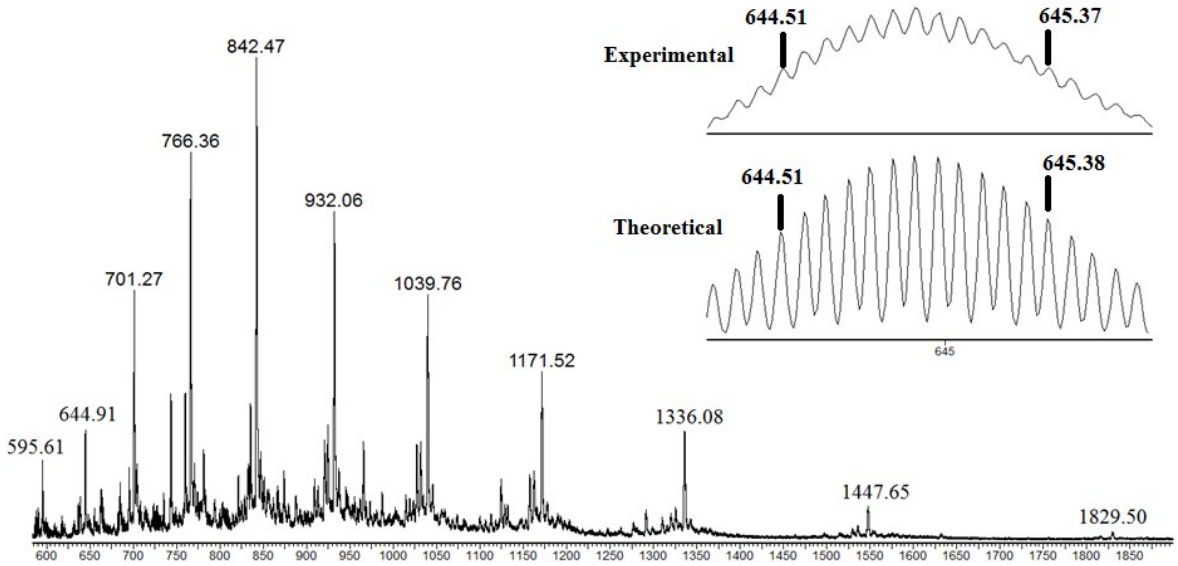

Figure S10. ESI-MS spectrum of cube **4** in MeCN (0.1 mg mL^{-1}).

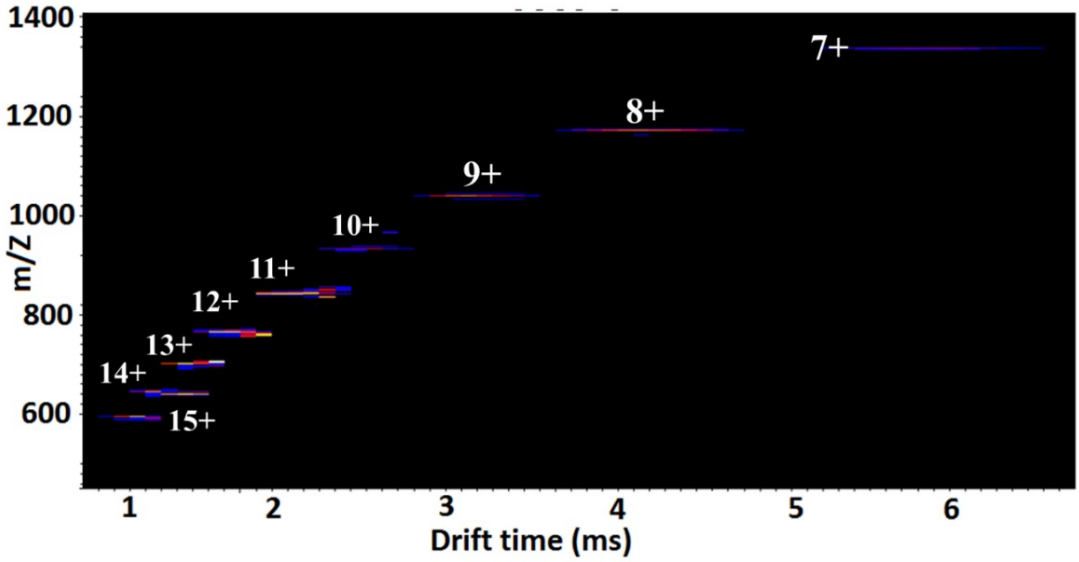

Figure S11. ESI-TWIM-MS spectrum of cube **4** in MeCN (0.1 mg mL^{-1}).

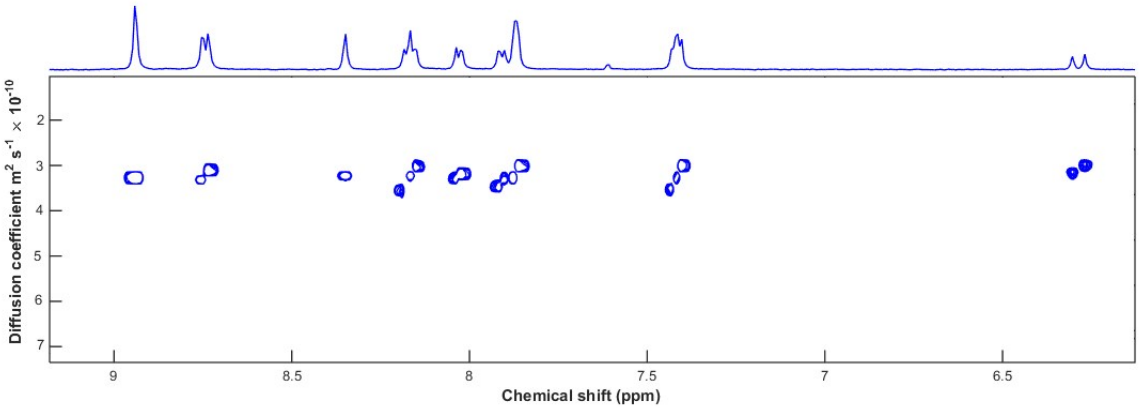

Figure S12. ^{1}H DOSY NMR spectrum of Cube **4** in CD_3CN.

The hydrodynamic radius was estimated according to the Stokes-Einstein Equation, where D is the diffusion constant, k is the Boltzmann constant, T is the temperature, μ is the viscosity of solvents, and r is the radius:

$$D = \frac{kT}{6\pi\mu r}$$

$D = 3.25\times10^{-10}\ m^2\ s^{-1}$

$k = 1.38\times10^{-23}\ N\ m\ K^{-1}$

$T = 298\ K$

$\mu = 3.45\times10^{-4}\ N\ m^{-2}\ s$ (CD_3CN)

$r = 1.94\times10^{-9}\ m = 1.94\ nm$

The hydrodynamic radius of the cubic complex **4** was determined to be 1.94 nm, which is consistent with the results of computer modeling.

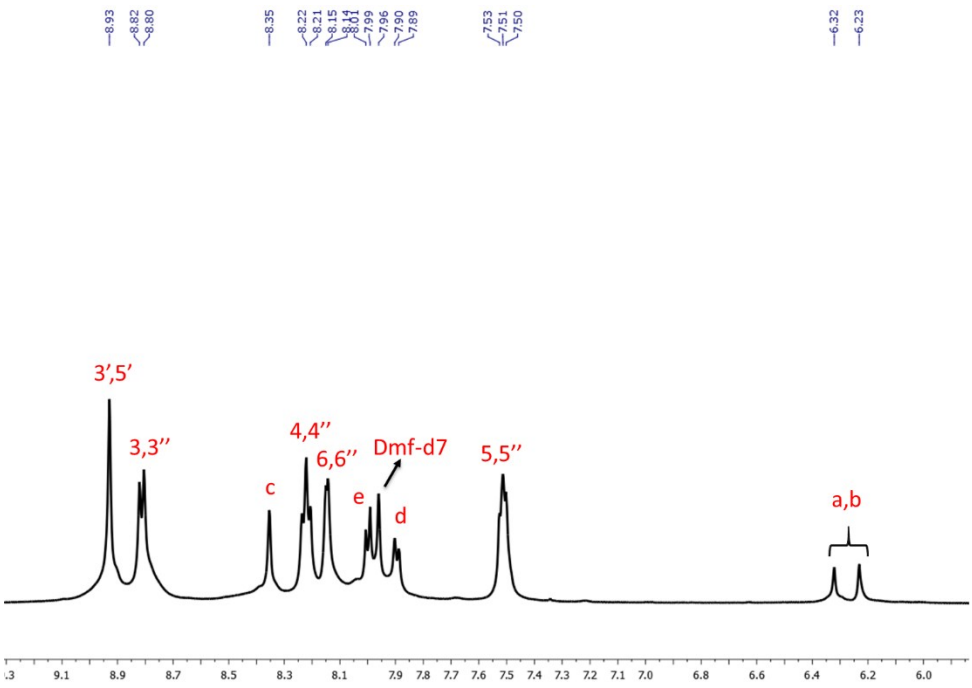

Figure S13. ^{1}H NMR spectrum (500 MHz, 300 K) of cube **5** in CD_3CN/DMF-d_7 (5:1 v/v).

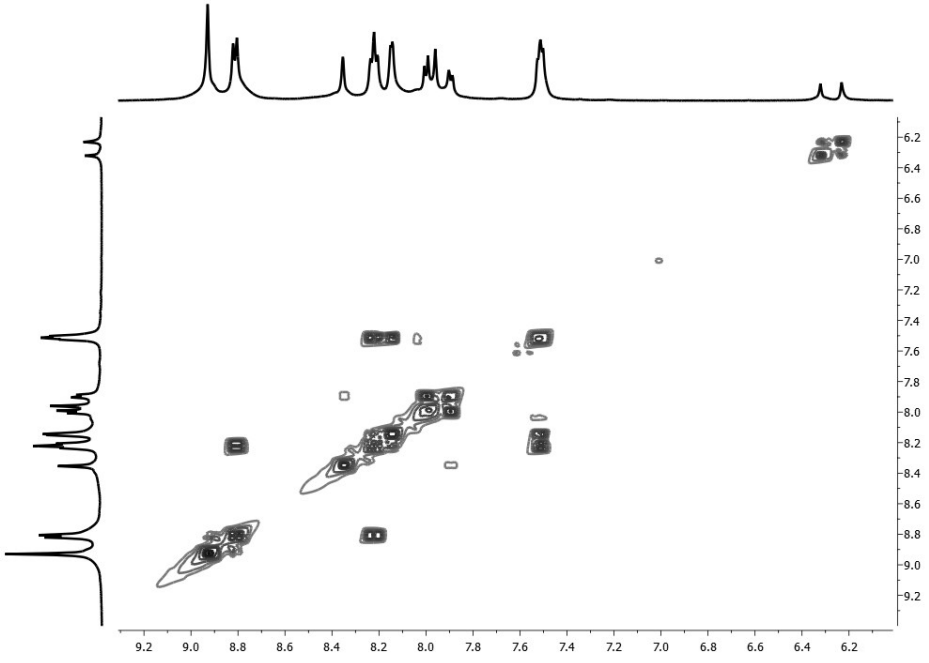

Figure S14. 2D COSY NMR spectrum of cube **5** in CD_3CN.

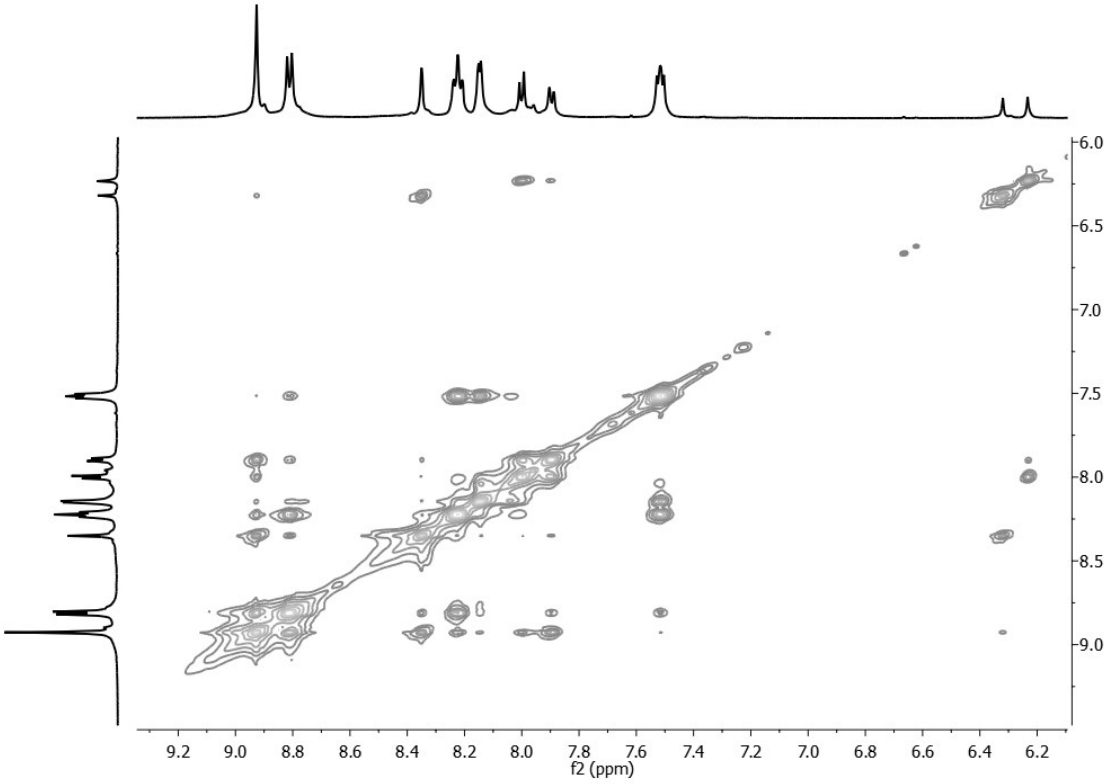

Figure S15. 2D NOESY NMR spectrum of cube **5** in CD_3CN.

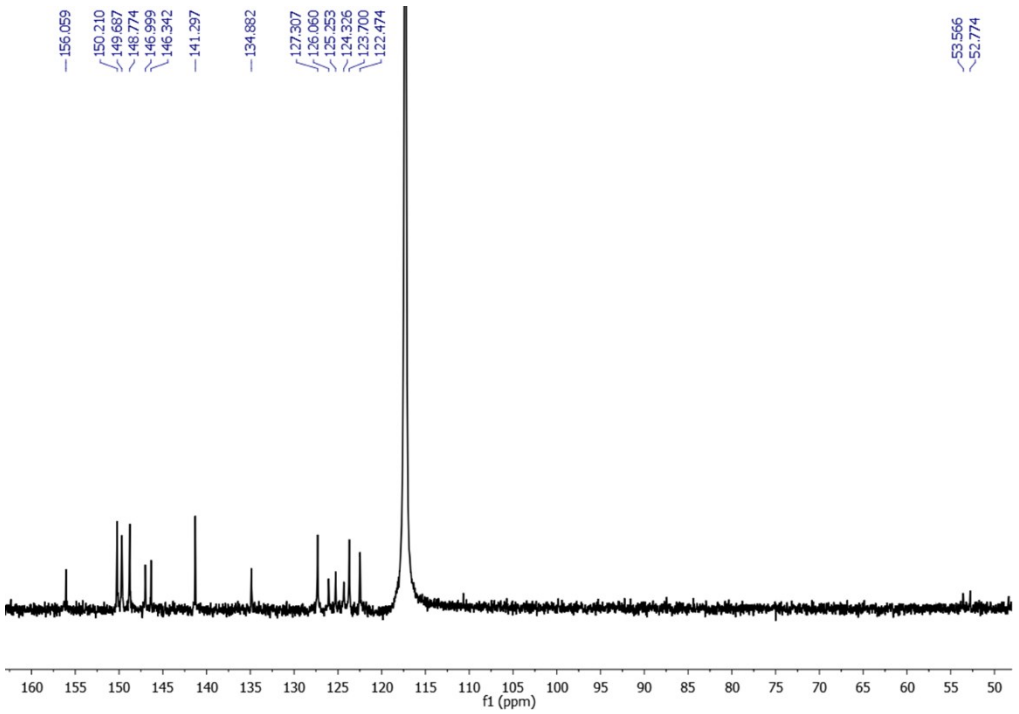

Figure S16. ^{13}C NMR spectrum (125 MHz, 300 K) of cube **5** in CD_3CN.

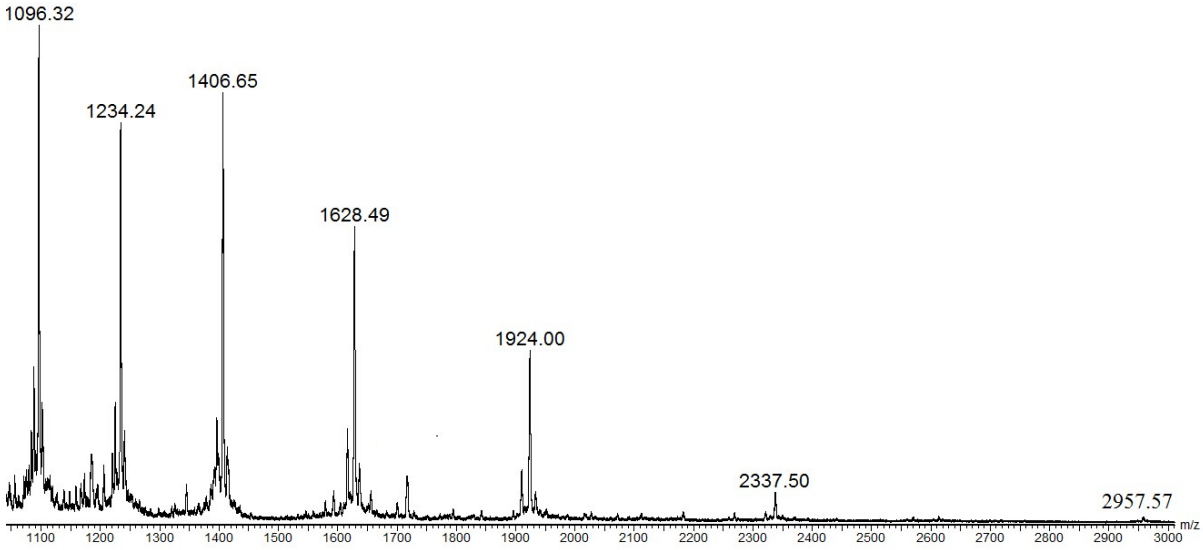

Figure S17. ESI-MS spectrum of cube **5** in MeCN.

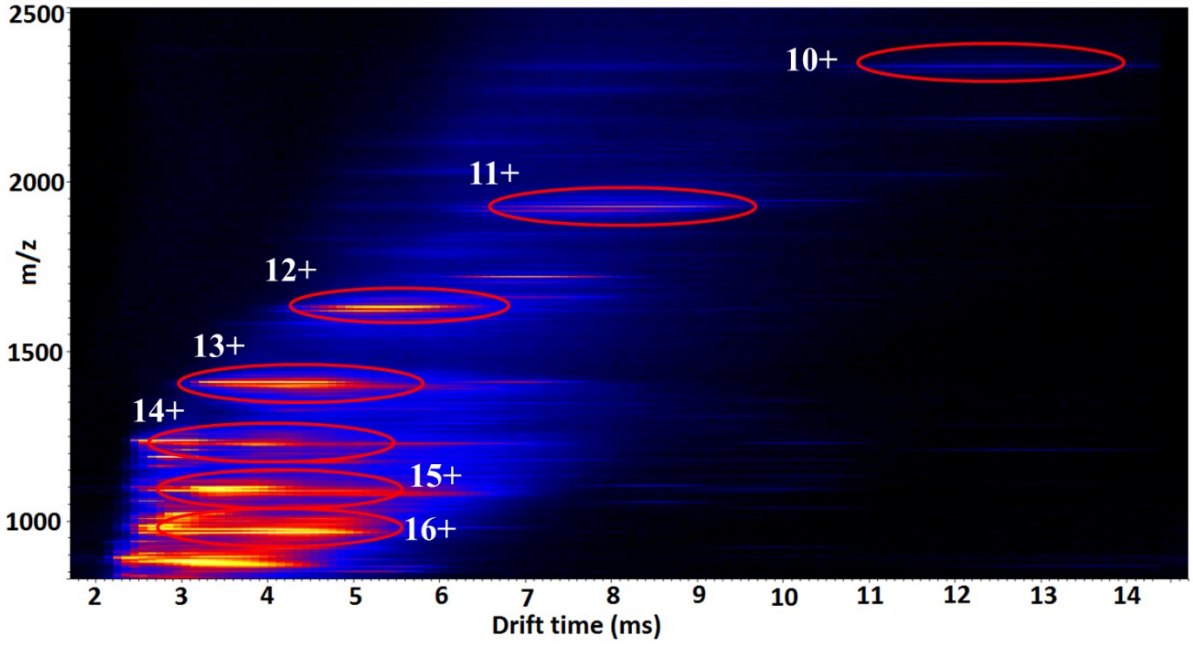

Figure S18. ESI-TWIM-MS spectrum of cube **5** in MeCN.

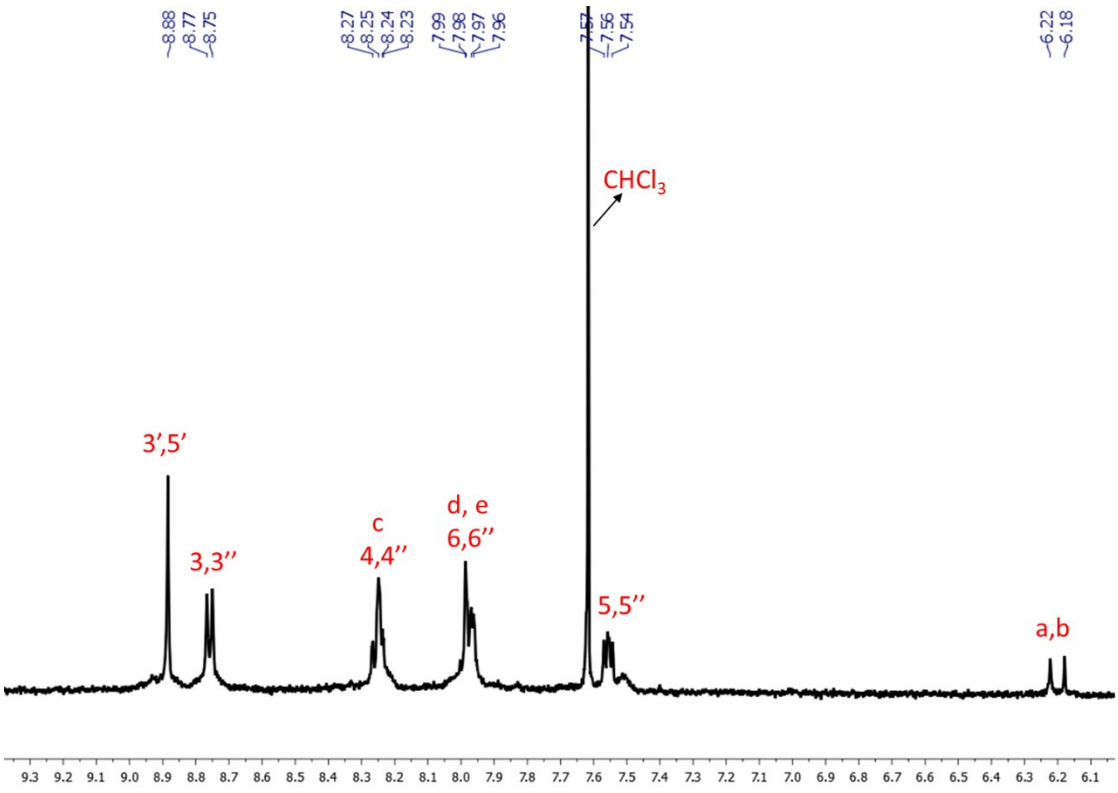

Figure S19. ^{1}H NMR spectrum (500 MHz, 300 K) of tetrahedron **7** in CD_3CN.

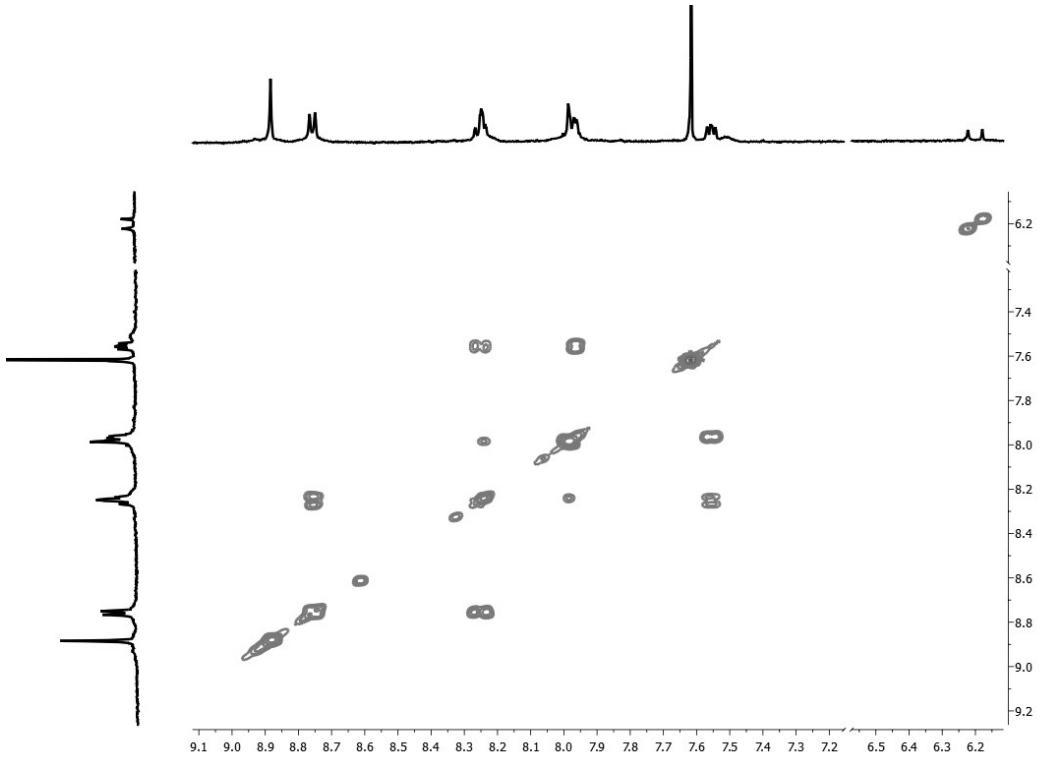

Figure S20. 2D COSY NMR spectrum of tetrahedron **7** in CD_3CN.

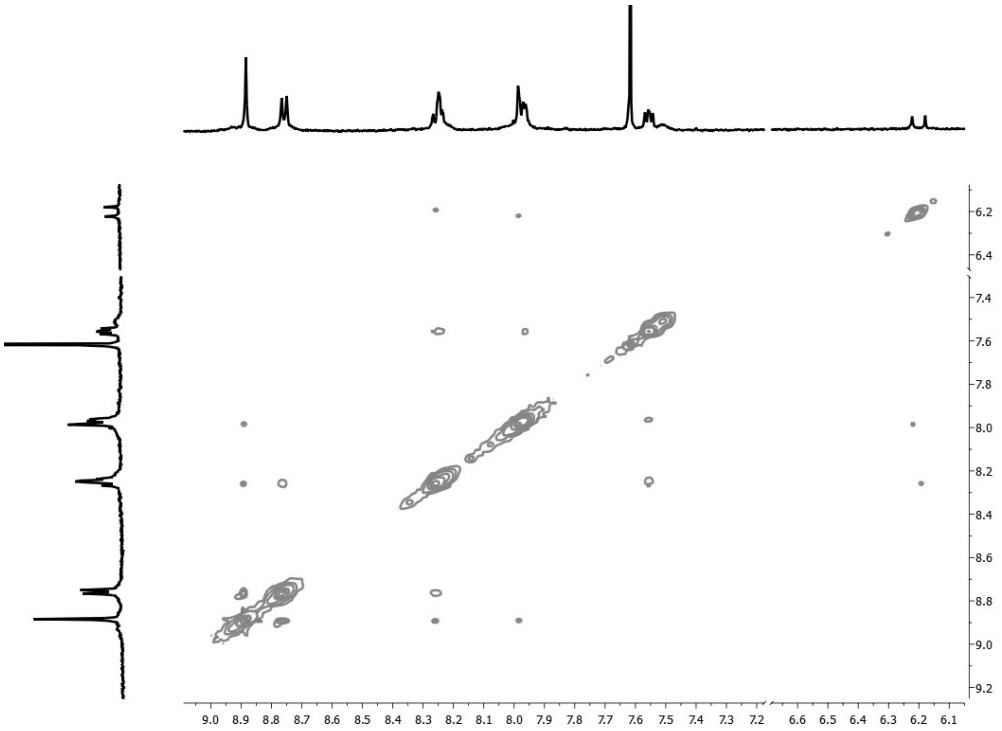

Figure S21. 2D NOESY NMR spectrum of tetrahedron **7** in CD_3CN.

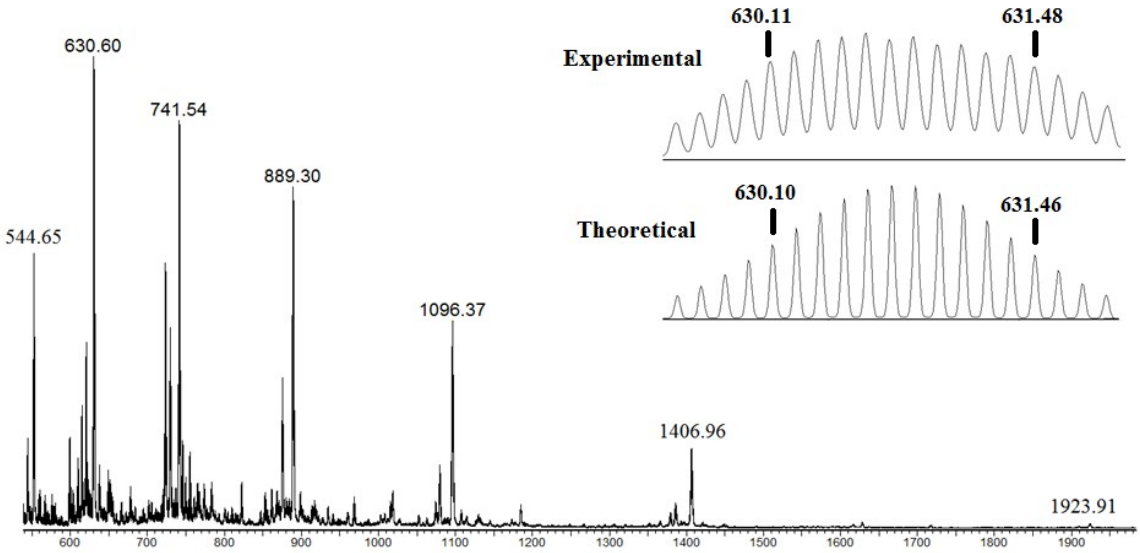

Figure S22. ESI-MS spectrum of tetrahedron **7** in MeCN.

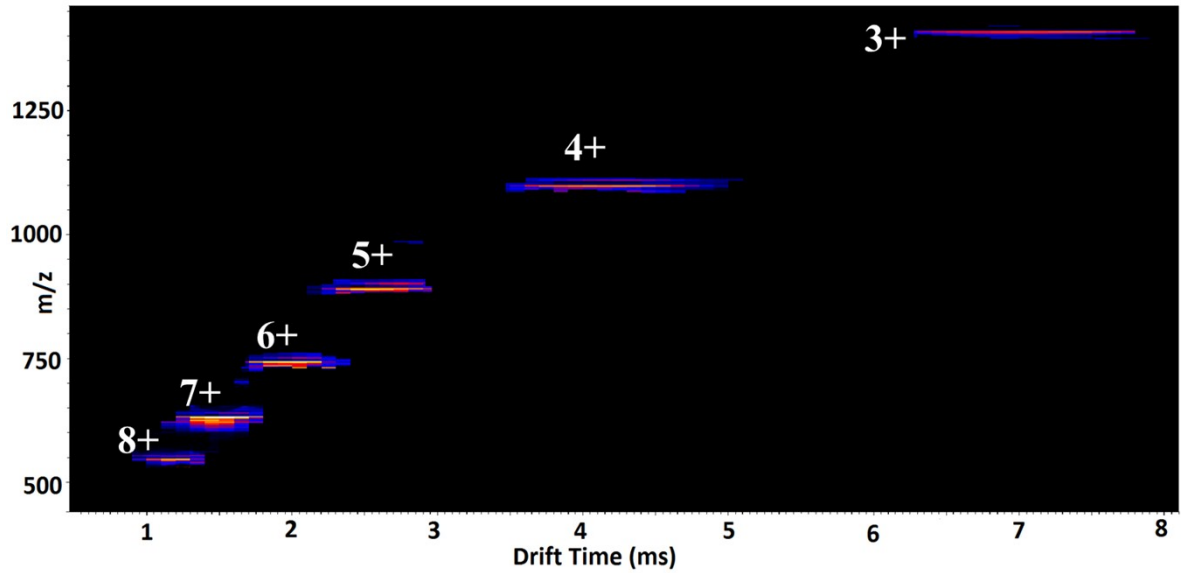

Figure S23. ESI-TWIM-MS spectrum of tetrahedron **7** in MeCN.

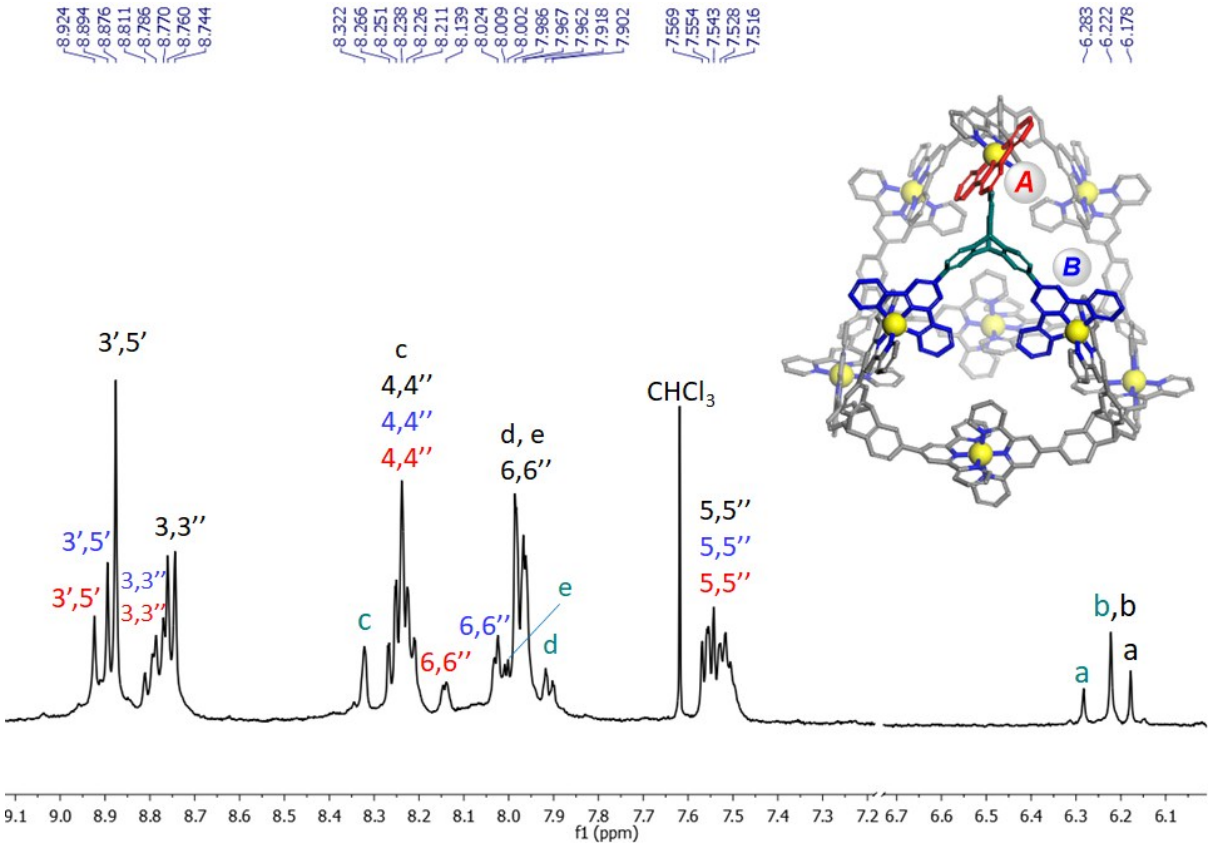

Figure S24. ^{1}H NMR spectrum of complexes **6** and **7** in CD_3CN (300 K, 500 MHz). The spectrum suggests a mixture of prism and tetrahedron conformers (red and blue, prism; black, tetrahedron).

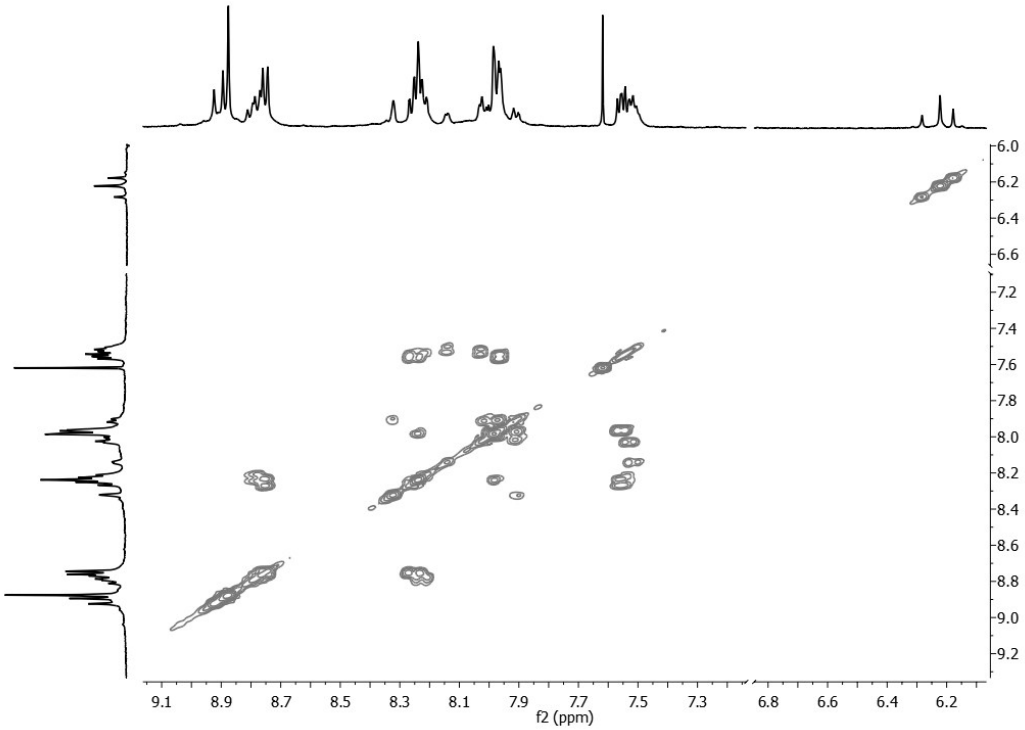

Figure S25. 2D COSY NMR spectrum of complexes **6** and **7** in CD_3CN.

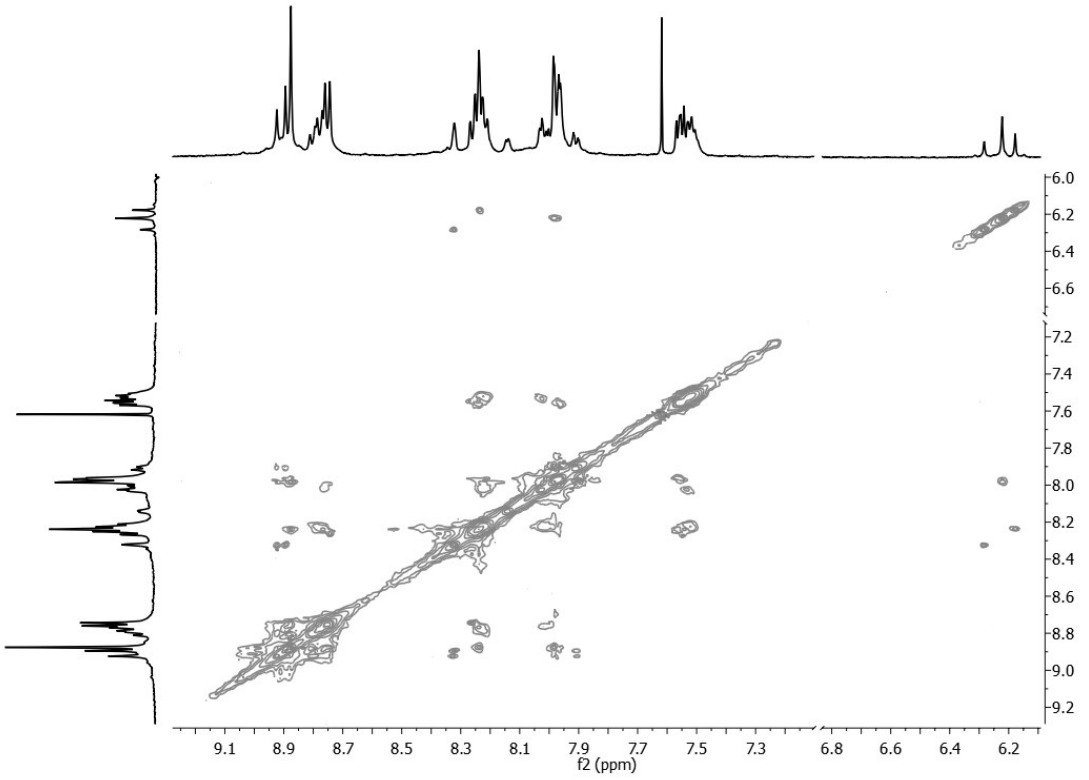

Figure S26. 2D NOESY NMR spectrum of complexes **6** and **7** in CD_3CN.

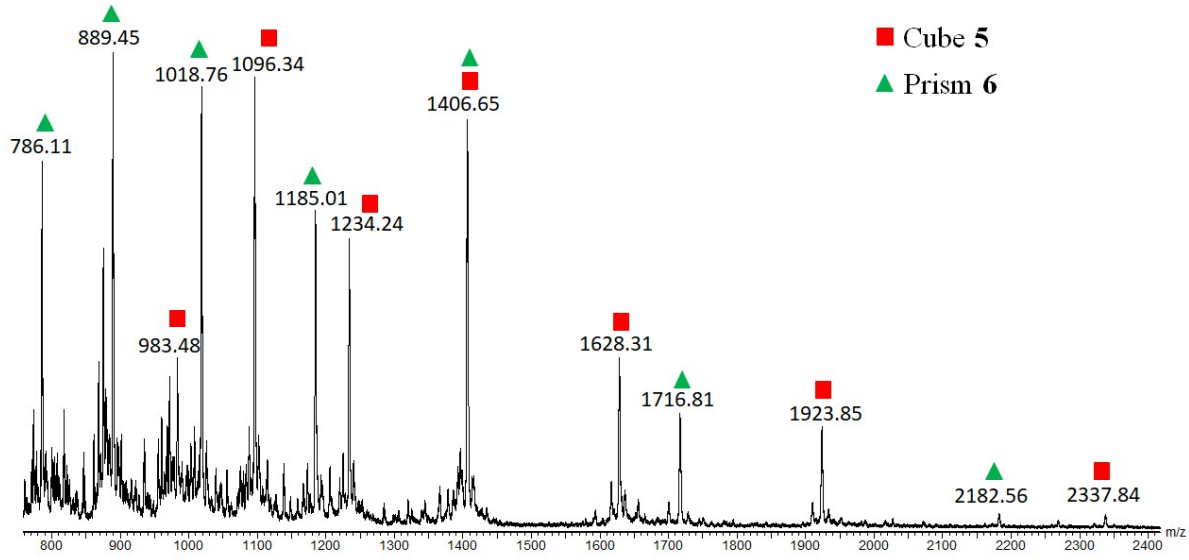

Figure S27. ESI-MS spectrum of cube **5** and prism **6** in MeCN.

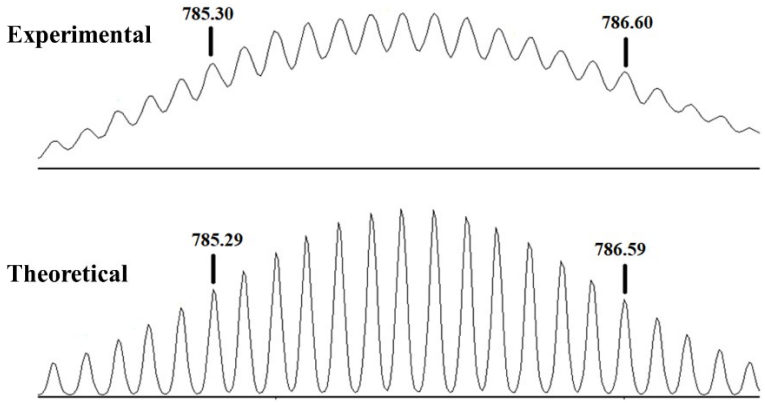

Figure S28. Isotopic distribution pattern and the simulated pattern of the 10+ charge state in ESI-MS spectrum of prism **6**.

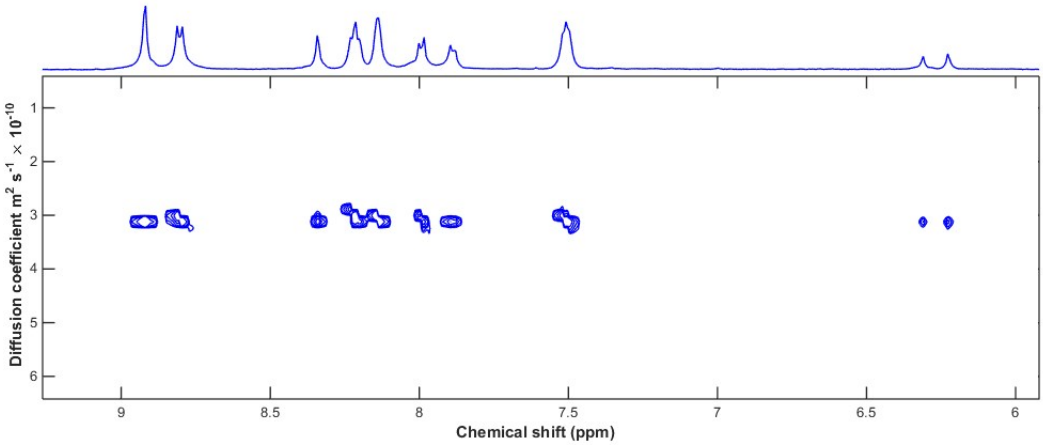

Figure S29. ^{1}H DOSY NMR spectrum of cube **5** in CD_3CN.

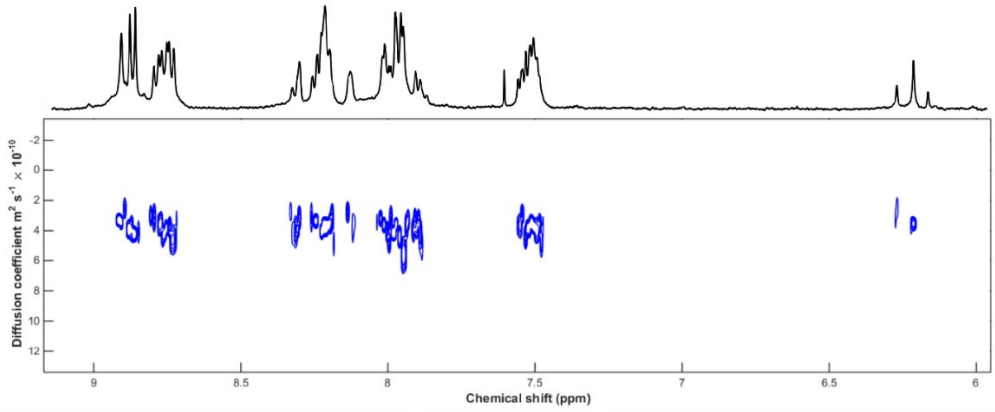

Figure S30. ^{1}H DOSY NMR spectrum of prism **6** and tetrahedron **7** in CD_3CN.

The hydrodynamic radius was estimated according to the Stokes-Einstein Equation, where D is the diffusion constant, k is the Boltzmann's constant, T is the temperature, μ is the viscosity of solvents, and r is the radius:

$$D = \frac{kT}{6\pi\mu r}$$

For complex **5**, $D = 3.19\times10^{-10}$ m^2 s^{-1}

$k = 1.38\times10^{-23}$ N m K^{-1}

$T = 298$ K

$\mu = 3.45\times10^{-4}$ N m^{-2} s (CD_3CN)

$r = 1.98\times10^{-9}$ m = 1.98 nm

The hydrodynamic radius of the cube **5** was determined to be 1.98 nm. Similarly, for prism **6** is 1.71 nm, and tetrahedron **7** is 1.59 nm, which are consistent with the results of computer modeling.

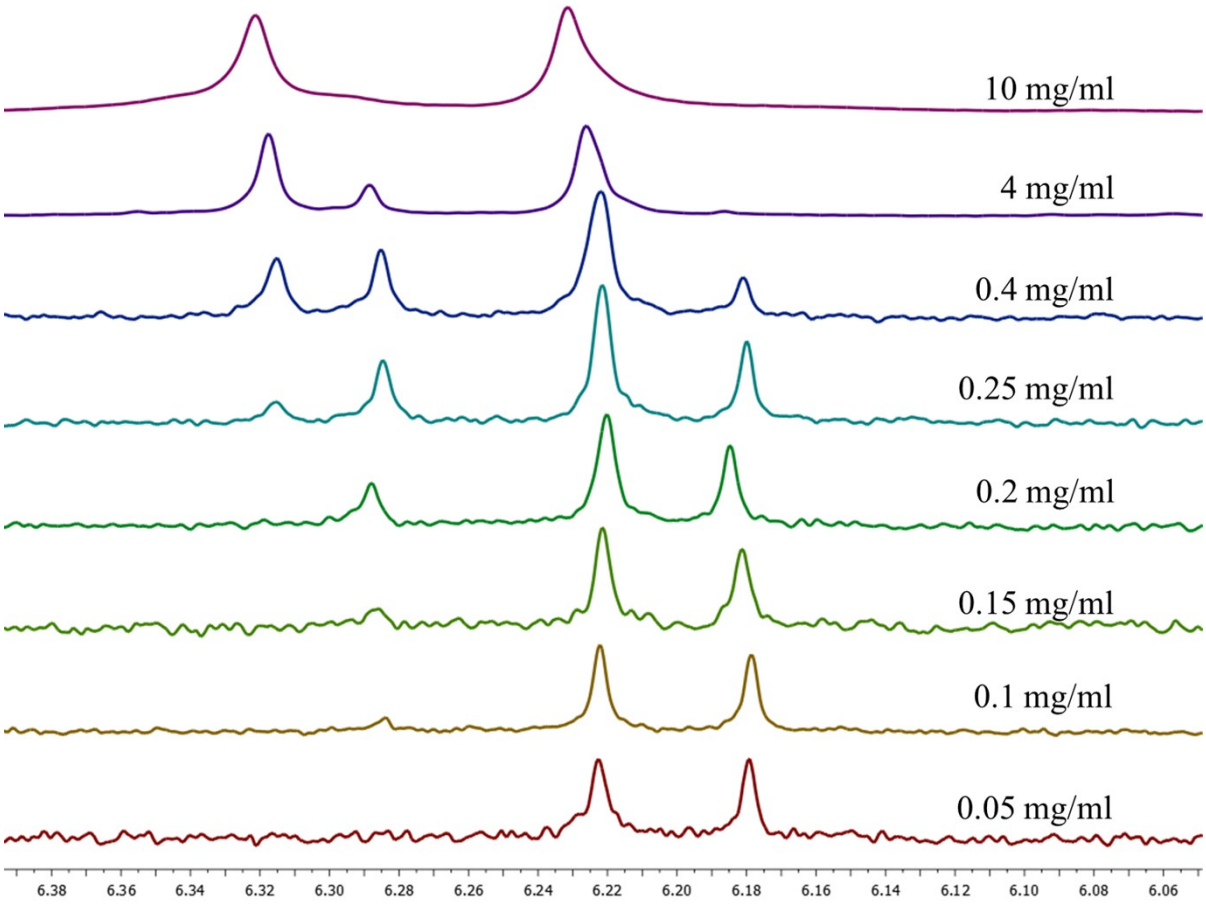

Figure S31. ^{1}H NMR spectra (bridge head protons only) of concentration dependent dynamic equilibrium of **5**, **6**, and **7** at 300 K in CD_3CN.

Calibration of drift time (t_D) scale and collision cross sections (CCS)

Table S1. Drift times and collision cross sections for the complex **4**

z	MW	m/z	t_D	Experimental CCS (Å^2)	Standard Deviation (Å^2)
5	11123.70	2224.74	11.73	1304	5.60
6	10978.74	1829.79	7.35	1248	4.29
7	10833.76	1547.68	4.77	1181	0.00
8	10688.80	1336.10	5.61	1461	13.18
9	10543.86	1171.54	4.05	1403	0.00
Total Average CCS				***1320***	***6.69***
Average Theoretical CCS				***1424***	

Table S2. Drift times and collision cross sections for the complex **5**					
z	**MW**	**m/z**	**t_D**	**Experimental CCS (Å²)**	**Standard Deviation (Å²)**
5	11688.05	2337.61	11.19	1275	8.58
6	11543.10	1923.85	7.55	1265	8.43
7	11398.10	1628.30	4.99	1207	6.11
8	11253.20	1406.65	4.06	1248	0.00
Total Average CCS				***1249***	***6.75***
Average Theoretical CCS (PA Method)				***1208***	

Table S3. Drift times and collision cross sections for the complex **6**					
z	**MW**	**m/z**	**t_D**	**Experimental CCS (Å²)**	**Standard Deviation (Å²)**
5	8584.85	1716.97	6.32	967	0.00
6	8439.90	1406.65	6.19	1148	4.69
Total Average CCS				***1058***	***3.31***
Average Theoretical CCS				***1125***	

Table S4. Drift times and collision cross sections for the complex **7**					
z	**MW**	**m/z**	**t_D**	**Experimental CCS (Å²)**	**Standard Deviation (Å²)**
4	48375.88	1406.65	6.41	778	0.00
Total Average CCS				***778***	***0.00***
Average Theoretical CCS				***757***	

All drift times (t_D) were collected at a traveling wave velocity of 350 m/s and a traveling wave height of 7.5 V.

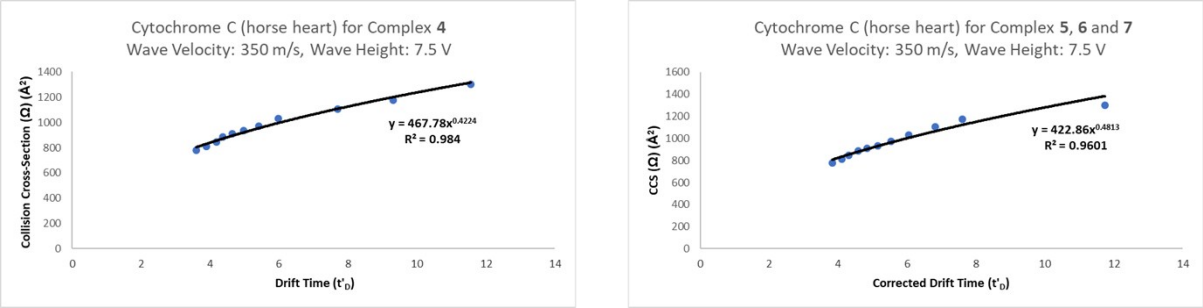

Figure S35. Calibration curve for the calibration of T-Wave drift time measurements.

Table S5: Cytochrome C Standard Collision Cross Section (CCS) calibration (Complex4)

z	MW	m/z	t_D (ms)	t'_D (ms)	Theoretical Ω (Å^2)	Ωc (Å2)
9	12363.50	1373.72	11.61	11.56	2215	1301
10	12364.50	1236.75	9.36	9.31	2226	1177
11	12365.50	1124.32	7.74	7.69	2303	1107
12	12366.50	1030.63	6.03	5.98	2335	1029
13	12367.50	951.35	5.46	5.42	2391	972
14	12368.50	883.47	5.01	4.97	2473	934
15	12369.50	824.64	4.68	4.64	2579	909
16	12370.40	773.15	4.41	4.37	2679	885
17	12372.30	727.78	4.23	4.19	2723	847
18	12374.10	687.45	3.93	3.89	2766	812
19	12375.60	651.35	3.63	3.59	2800	779

Table S6: Cytochrome C Standard Collision Cross Section (CCS) calibration (Complex 5, 6 and 7)

z	MW	m/z	t_D (ms)	t'_D (ms)	Theoretical Ω (Å^2)	Ωc (Å2)
9	12363.50	1373.72	11.79	11.74	2215	1301
10	12364.50	1236.75	7.65	7.60	2226	1177
11	12365.50	1124.32	6.87	6.82	2303	1107
12	12366.50	1030.63	6.09	6.04	2335	1029
13	12367.50	951.35	5.58	5.54	2391	972
14	12368.50	883.47	5.19	5.15	2473	934
15	12369.50	824.64	4.89	4.85	2579	909
16	12370.40	773.15	4.62	4.58	2679	885
17	12372.30	727.78	4.35	4.31	2723	847
18	12374.10	687.45	4.14	4.10	2766	812
19	12375.60	651.35	3.87	3.83	2800	779

Table S7: Crystal data and structure refinement for 4.	
Identification code	**4**
Empirical formula	$C_{520}H_{328}N_{72}Zn_{12}$
Formula weight	8368.96
Temperature/K	100.15
Crystal system	cubic
Space group	F-43c
a/Å	60.721(8)
b/Å	60.721(8)
c/Å	60.721(8)
α/°	90
β/°	90
γ/°	90
Volume/Å^3	223885(90)
Z	8
ρ_{calc}g/cm^3	0.497
μ/mm^{-1}	0.069
F(000)	34496.0
Crystal size/mm^3	0.06 × 0.06 × 0.06
Radiation	synchrotron (λ = 0.44281)
2Θ range for data collection/°	1.672 to 21.262
Index ranges	-50 ≤ h ≤ 50, -50 ≤ k ≤ 50, -50 ≤ l ≤ 50
Reflections collected	414715
Independent reflections	5665 [R_{int} = 0.1119, R_{sigma} = 0.0233]
Data/restraints/parameters	5665/1186/454
Goodness-of-fit on F^2	1.097
Final R indexes [I>=2σ (I)]	R_1 = 0.0996, wR_2 = 0.2558
Final R indexes [all data]	R_1 = 0.1002, wR_2 = 0.2567
Largest diff. peak/hole / e Å^{-3}	0.21/-0.43
Flack parameter	0.461(11)

References

[1] K. Thalassinos, M. Grabenauer, S. E. Slade, G. R. Hilton, M. T. Bowers, J. H. Scrivens, *Anal. Chem.* 2009, **81**, 248-254.

[2] F. A. Fernandez-Lima, R. C. Blas, D. H. Russell, *Int. J. Mass Spectrom.* 2010, **298**, 111-118.

[3] Bruker (2016) APEX3 (Version 2015.9). Bruker AXS Inc., Madison, Wisconsin, USA.

[4] Bruker (2016) SAINT V8.35A. Data Reduction Software.

[5] G. M. Sheldrick, SADABS. Program for Empirical Absorption Correction, University of Gottingen, Germany, 1996.

[6] G. M. Sheldrick, SHELXL-97. Program for the Refinement of Crystal, 1997.

[7] G. M. Sheldrick, *Acta Cryst*. 1990, **A46**, 467-473

[8] G. M. Sheldrick, *Acta Cryst*. 2008, **A64**, 112-122.

[9] O. V. Dolomanov, L. J. Bourhis, R. J. Gildea, J. A. K. Howard, H. Puschmann, *J. Appl. Cryst*. 2009, **42**, 339-341

[10] A. L. Spek, *Acta Cryst*. 1990, **A46**, 194-201.

[11] A. L. Spek, *Acta Cryst*. 1990, **A46**, c34.

[12] C. Zhang, C.-F. Chen, *J. Org. Chem*., 2006, **71**, 6626.

[13] M. Schmittel, B. He, P. Mal *Org. Lett*., 2008, **10**, 2513-2516.